Biogeosciences Discuss., 9, 3003–3030, 2012
www.biogeosciences-discuss.net/9/3003/2012/
doi:10.5194/bgd-9-3003-2012

Biogeosciences Discussions

Observed trends of anthropogenic acidification in North Atlantic water masses

M. Vázquez-Rodríguez[1], F. F. Pérez[1], A. Velo[1], A. F. Ríos[1], and H. Mercier[2]

[1]Department of Oceanography, Instituto de Investigaciones Marinas (IIM), CSIC, Eduardo Cabello 6, 36208 Vigo, Spain
[2]Laboratoire de Physique des Océans (LPO), CNRS Ifremer IRD UBO, IFREMER Centre de Brest, B.P. 70 29280 Plouzané, France

Received: 29 February 2012 – Accepted: 4 March 2012 – Published: 14 March 2012

Correspondence to: M. Vázquez-Rodríguez (mvazquez@iim.csic.es)

Published by Copernicus Publications on behalf of the European Geosciences Union.

Abstract

The lack of observational pH data has made difficult assessing recent rates of ocean acidification, particularly in the high latitudes. Here we present a time series of high-quality carbon system measurements in the North Atlantic, comprising fourteen cruises spanning over 27 yr (1981–2008) and covering important water mass formation areas like the Irminger and Iceland basins. We provide direct quantification of anthropogenic acidification rates in upper and intermediate North Atlantic waters by removing the natural variability of pH from the observations. Bottle data were normalised to basin-average conditions using climatological data and further condensed into averages per water mass and year to examine the temporal trends. The highest acidification rates of all inspected water masses were associated with surface waters in the Irminger Sea ($-0.0018 \pm 0.0001\ yr^{-1}$) and the Iceland Basin ($-0.0012 \pm 0.0002\ yr^{-1}$) and, unexpectedly, with Labrador Seawater (LSW) which experienced an unprecedented pH drop of $-0.0015 \pm 0.001\ yr^{-1}$. The latter stems from the formation by deep convection and the rapid propagation in the North Atlantic subpolar gyre of this well-ventilated water mass. The high concentrations of anthropogenic CO_2 are effectively transported from the surface into intermediate waters faster than via downward diffusion, thus accelerating the acidification rates of LSW. An extrapolation of the observed lineal trends of acidification suggests that the pH of LSW could drop 0.45 units with respect to pre-industrial levels by the time atmospheric CO_2 concentrations double the present ones.

1 Introduction

The chemistry behind ocean acidification is well known and researched (Doney et al., 2009; Raven et al., 2005), but the accurate tracking of its recent evolution remains widely uncertain due to the sparseness and varying quality of field data (Byrne et al., 2010; Tittensor et al., 2010; Wootton et al., 2008). Roughly 20–35 % of the excess anthropogenic CO_2 in the atmosphere is quenched by the oceans (Khatiwala et

BGD
9, 3003–3030, 2012

al., 2009) and this helps hampering global warming and mitigating climate change. But when CO_2 dissolves in seawater carbonic acid (H_2CO_3) forms and hydrogen ions (H^+) are released to the aqueous phase, lowering pH, carbonate ion concentrations ($[CO_3^{2-}]$) and causing the so-called "ocean acidification". Since the beginning of the Industrial Revolution in 1780's the sea-surface's has seen a 30 % reduction on pH (0.1 units; Caldeira and Wickett, 2005; Raven et al., 2005). The current acidification episode is occurring ~100 times faster than any other acidity change in the last 300 million years of Earth's history (Pelejero et al., 2010; Hönisch et al., 2012), and it is the onset for a number of cascading effects throughout marine ecosystems that may leave no time for adaptation of many organisms (Feely et al., 2008; Doney et al., 2009). Ocean acidification has a medley of juxtaposed, but mostly deleterious impacts on the aquatic environment (Doney et al., 2009): from reproductive, larval survivorship and growth-related issues in several taxa to the reduction of seawater's sound absorption coefficient (Ilyina et al., 2009).

The North Atlantic Subpolar Gyre (NASPG) has been nicknamed "the bellwether" of ocean acidification and urged to be closely monitored (Fabry et al., 2009). It has a low buffering capacity (high Revelle Factor; Sabine et al., 2004), meaning that the same amount of CO_2 added to it causes a greater pH reduction than in tropical waters that have higher buffering capacity. Due to the deep convection in the Irminger and Iceland basins (Azetsu-Scott et al., 2003; Pérez et al., 2010) (Fig. 1a) the water mass formation processes abound (surface seawater undergoing cooling and/or haline transformations, gaining density, sinking and eventually mixing) and turn the NASPG into the most effective entrance portal of human-produced CO_2 into the ocean (Sabine et al., 2004). The negative feedback is that as the ocean takes up anthropogenic CO_2 the pH and the buffering capacity decrease, thus degrading the ocean's ability to keep up with the absorption of atmospheric CO_2 (Friedlingstein et al., 2006; Friedlingstein and Prentice, 2010).

There are relatively few spots where the carbon system has been surveyed thoroughly enough to generate a comprehensive database that can be used in the

BGD
9, 3003–3030, 2012

assessment of ocean acidification and its environmental impacts (Wootton et al., 2008). Several past and future pH projections have been proposed from Ocean General Circulation Models (GCMs) and synthetic ocean data (Orr et al., 2005), but empirical data documenting the evolution of ocean pH over time are limited (Wootton et al., 2008; Hönisch et al., 2012). The present work examines the temporal variability of pH in the main water masses of the North Atlantic, as well as its drivers, from direct observations. Here we have gathered the available high-quality, NASPG-covering carbon system data between 1981 and 2008 (Fig. 1a) to study the decadal acidification rates of the main North Atlantic water masses (Fig. 1b) during that time period.

2 Dataset and methodology

2.1 Dataset

The relatively recent introduction of spectrophotometric pH determination (Clayton and Byrne, 1993) allowed making fast and yet very accurate shipboard pH measurements, filling the need of improving and enlarging the observational datasets against which predictive numerical models are built and synthetic data gets tested (Tittensor et al., 2010; Sabine et al., 2004). A total of fourteen cruises with high-quality carbon system measurements were selected to follow the temporal evolution of pH in the North Atlantic. The combined dataset spans over 27 yr (1981–2008) and gives a comprehensive spatial coverage of the study area (Fig. 1a; Table 1), with an emphasis on important water mass formation areas like the Irminger and Iceland basins. The geographical boundaries of the Irminger basin have been established taking the main longitudinal axis of the Reykjanes Ridge and the southeast coast of Greenland (Fig. 1a). The Iceland basin is defined as the region enclosed between the Reykjanes ridge axis and the line joining the Eriador Seamount and the Faroe Islands. The region designated as Eastern North Atlantic basin (ENA basin hereinafter) extends south from the Eriador-Faroe line over the Rockall trough, the Porcupine bank, and the Biscay and Iberian

BGD
9, 3003–3030, 2012

basins. Cruise data here used can be accessed at the Carbon In the Atlantic (CARINA) data portal http://store.pangaea.de/Projects/CARBOOCEAN/carina/index.htm. The climatological WOA05 data is available at http://www.nodc.noaa.gov/OC5/WOA05/pr_woa05.html

The pH measurements compiled in our dataset have a variety of different analytical procedures, depending on the cruise, and the same applies to precision limits (Table 1). Only bottle data of the inorganic carbon system was used and all measurements are compliant with the latest carbon system analytical recommendations for seawater (Dickson et al., 2007). The pH measurements in the database were determined either potentiometrically (using pH electrodes; Dickson, 1993) or, more commonly, with a spectrophotometric method that used *m*-cresol purple as a pH indicator in either scanning or diode array spectrophotometers (Clayton and Byrne, 1993). The spectrophotometric pH determination has typical reported precision limits of 0.002 pH units (Clayton and Byrne, 1993; Millero, 2007). Exceptionally, the pH measurement protocols of the FOUREX and OVIDE cruises (Table 1) included periodical checks with CRMs (Certified Reference Material for seawater carbon system analytics) that allowed achieving even lower precisions. All pH measurements that had not been originally reported in the seawater scale (pH_{SWS}; Millero, 2007) were converted to it from either the total or the free pH scale (pH_T and pH_F, respectively; Millero, 2007) using the corresponding acid dissociation constants (HF or HSO_4^-). The SWS uses calibration buffer solutions that are closest in composition to natural seawater and its definition includes H^+ associated with fluoride and sulphate so that errors associated with the HF or HSO_4^- dissociation constants are avoided (Friis et al., 2004). The use of a single common scale prevents discrepancies of up to 0.01 pH units in samples of identical acidity. For simplicity, pH_{SWS} is denoted as pH in this study.

Some of the cruises listed in Table 1 did not perform direct pH measurements but obtained total alkalinity (A_T) and dissolved inorganic carbon (C_T) data. In such cases the pH values were calculated from A_T and C_T data using the thermodynamic equations of the carbon system (Dickson et al., 2007) and a set of carbon dioxide dissociation

BGD
9, 3003–3030, 2012

constants (Dickson and Millero, 1987). The estimated accuracy for these particular pH values is ±0.0034. The shipboard total alkalinity (A_T) was analysed with potentiometric titration and determined by developing either a full titration curve (Millero et al., 1993; Dickson et al., 2007) or from single point titration (Pérez and Fraga, 1987; Mintrop et al., 2002). Dissolved inorganic carbon (C_T) samples were analysed with Single Operator Multiparameter Metabolic Analysers (SOMMA apparatus) based on coulometric titration techniques (Johnson et al., 1993), and were calibrated with CRMs. The exception is the 1981 TTO cruise, where C_T was determined potentiometrically (Bradshaw et al., 1981) and no CRMs were used. The analytical accuracies for C_T and A_T were typically assessed within ±2 µmol·kg^{-1} and ±4 µmol·kg^{-1}, respectively. Unless otherwise specified on Table 1, the preliminary results from a crossover analysis of Atlantic cruises performed by the CARBOOCEAN Atlantic Synthesis group sustain that no other corrections are needed in the dataset here used.

The A16N cruise performed on board spectrophotometric pH measurements, but the spatial resolution was worse than for C_T and A_T, so we used pH values calculated from C_T and A_T for this cruise instead. The AR07E and A01E cruises (Fig. 1a) were kept in the database because of their convenient geographic position in the context of this study, their timely date and comprehensive amount of C_T measurements, in spite of the very few potentiometric A_T data they reported. To improve their coverage of A_T values we obtained a regression of normalized A_T ($NA_T = A_T \cdot 35/S$, where "S" denotes salinity) vs. silicate concentration ($NA_T = 2294.7 + 1.37\ [Si(OH)_4]$; $R^2 = 0.97$ and standard deviation of residuals of ±3.7 µmol·kg^{-1}). This practice is justified and supported given the low variability of A_T in the North Atlantic (Friis et al., 2005). The obtained equation was applied to the AR07E and A01E datasets to generate A_T values at the same bottle depths with measured C_T data. The pH was then calculated from C_T and A_T data using the thermodynamic equations of the carbon system, as mentioned above.

BGD
9, 3003–3030, 2012

2.2 pH data analysis

2.2.1 Water mass approach

The sequestration of anthropogenic CO_2 in the NASPG is exceptionally intense due to the high convective activity and associated water mass formation events in this region. This induces important shifts in the inorganic carbon chemistry of the water masses involved (Azetsu-Scott et al., 2003; Pérez et al., 2008, 2010; Yashayaev et al., 2008). These particularities motivated a "water mass approach" to study the acidification processes and rates of the NASPG. The approach considers the individual water masses present in a region (Fig. 1b) and follows the temporal variability of their carbon system parameters. This same strategy has been successfully used in the past by various authors (Kieke et al., 2007; Pérez et al., 2008, 2010), including in the NASPG, and has the advantage of avoiding all the mixing problems common in closed volume and basin-wide approaches that encapsulate and treat equally very different water masses. Different boundary isopycnals were selected in the Irminger, Iceland and Eastern North Atlantic basins, ad hoc (Fig. 1b) to optimise the demarcation of the main NASPG water masses. To be consistent with the existing literature, the potential density limits (σ, in $kg\,m^{-3}$) suggested in several works (Kieke et al., 2007; Yashayaev et al., 2008) for the water masses here considered were adapted to our thermohaline field, whenever possible.

2.2.2 Normalization and averaging of pH data

The rates of anthropogenic acidification were calculated from in situ pH data after removing the natural variability component. Bottle data were normalised to basin-average conditions calculated from climatological data (WOA05: temperature, salinity, oxygen and nutrients) and the information was further condensed into averages per water mass and year so they could be plotted conveniently vs. time. This practice aims to avoid potential data representativeness biases derived from the low sampling resolution in relatively large areas, particularly in the Iceland and North ENA basins.

BGD
9, 3003–3030, 2012

The main factors that modulate the natural variability of ocean pH on decadal timescales need to be removed from observations in order to isolate and evaluate the anthropogenic forcing and its effects in ocean acidification. The pH of a particular body of water can naturally change due to water mass ventilation or mixing with other water parcels that have different pH signatures. Water mass mixing can be evaluated from θ and S relationships. In the NASPG it is also worth considering the signature [$Si(OH)_4$] peak of Antarctic waters to improve estimates of mixing proportions between Arctic and Antarctic water masses in mid and deep Atlantic layers (Pérez et al., 2010; Vázquez-Rodríguez et al., 2012). On the other hand, ventilation in the North Atlantic can be accurately traced by considering the apparent oxygen utilization term ($AOU = O_2^{sat} - O_2^{meas}$; where O_2^{sat} = saturation concentration of dissolved O_2; O_2^{meas} = measured concentration of dissolved O_2) and atmospheric molar fraction of CO_2 (xCO_2^{atm}) (Pérez et al., 2008). The anthropogenic and natural air-sea CO_2 fluxes have a large effect on ocean pH (Raven et al., 2005; Fabry et al., 2009), so the spatiotemporal variability of xCO_2^{atm} must be considered, particularly in the ocean layer affected by the mean penetration depth (MPD) of this gas, i.e., the uppermost 500 m (on average) in North Atlantic waters (Pérez et al., 2010).

The above-mentioned elements were calculated applying MLR fits to cruise data and expressed as individual pH correction elements (ΔpH_c) for each cruise, water mass and basin as follows:

$$\Delta pH_c = \sum_{i=1}^{4} a_i \left(X_i^{WOA05} - X_i^{c} \right) \quad (1)$$

Where "c" stands for "cruise" and subscript "i" denotes "property" ($1 = Si(OH)_4$; $2 = AOU$; $3 = \theta$; $4 = S$). The "X_i^{c}" and "X_i^{WOA05}" terms are the average magnitudes of the "ith" properties from direct observations and from WOA05 data, respectively (Supplement: Tables S1 through S3). The "X_i^{WOA05}" terms are taken as references of average conditions in the corresponding water masses and basins. The "a_i" factors are the regression coefficients that were obtained from another MLR

BGD
9, 3003–3030, 2012

fit (Eq. 2) of the corresponding pH average (for each water mass and basin) vs. the "i" properties (Tables S1 through S3 in the Supplement). The obtained "a_i" regression coefficients are listed in Table 2.

$$pH_{MLR} = \sum_{i=1}^{5} a_i X_i + k \quad (2)$$

All terms and scripts in the above pH_{MLR} equation have the same meaning as in Eq. (1). The $X_5 = xCO_2^{atm}$ values used as input parameters in Eq. (2) are the averages for the year of the corresponding cruise "c". The xCO_2^{atm} records were obtained from time series of selected meteorological stations of the global cooperative air-sampling network, managed and operated by the National Oceanic and Atmospheric Administration (NOAA) Carbon Cycle Greenhouse Gas group (http://www.esrl.noaa.gov/gmd/ccgg/flask.html).

The a_5 terms associated with the xCO_2^{atm} explanatory variable (Table 2) in Eq. (2) are not used in Eq. (1). Such terms are only necessary when calculating the "a_i" coefficients from Eq. (2). Having "a_5" included in the pH_{MLR} expression removes from the rest of "a_i" the influences of the time-dependant xCO_2^{atm} variable, which certainly co-varies with pH and is, in fact, the relationship that we are interested in examining. By doing so, the ΔpH_c expression remains as an approximation that explains only the spatial variability of pH, as intended originally.

By doing the above calculations the pH averages can be seasonally and spatially detrended, referenced to average climatological conditions and to the corresponding xCO_2^{atm} of the year each cruise "c" was conducted ("pH_c" in Tables S1 through S3). This is achieved by applying the following linear approximation:

$$pH_c* = pH_c + \Delta pH_c \quad (3)$$

The calculated ΔpH_c are generally close to zero in the deep layers and tend to have larger values in recently ventilated waters and in the surface. The order of magnitude of the ΔpH_c terms is $\sim 10^{-3}$, meaning that their contribution to the overall variability of

BGD
9, 3003–3030, 2012

pH is rather modest considering the raw spatiotemporal differences observed in Fig. 2 (or Supplement, Tables S1 through S3). The average ΔpH_c for the Irminger basin was estimated in $(11 \pm 9) \times 10^{-3}$. It is the largest average ΔpH_c in this study, compared with the $(3 \pm 9) \times 10^{-3}$ and $(1 \pm 10) \times 10^{-3}$ values obtained for the Iceland and ENA basins, respectively. The residual correlation between the natural and anthropogenic components of pH can only represent a minor part of the already small ΔpH_c term and have a very small weight in pH_c*.

3 Results

As a first approximation to the evolution of pH over the last two decades, the vertical distributions of pH along sections between the Iberian Peninsula and Greenland are shown (Fig. 2). The general patterns of measured pH follow the expected natural distributions: the high pH values above the seasonal thermocline, in the photic layer (uppermost ~400 m), respond to the photosynthetic activity of primary producers that withdraw dissolved CO_2 from seawater. Deeper and older layers (like North Atlantic Deep Water, NADW; Fig. 1b) are naturally more acidic because they are less ventilated than surface waters, have lower dissolved oxygen concentrations and larger amounts of dissolved inorganic carbon coming from the remineralization (oxidation) of particulate and dissolved organic matter. Nonetheless, this pH drop in old waters is slightly buffered by the high normalized A_T ($NA_T = A_T \cdot 35/S$) that neutralizes acidic species, particularly below the lysocline (>2300 dbar on average for these regions), at the high pressure and low temperature conditions of the deep ocean (Feely et al., 2004). However, this neutralisation occurs over century or longer timescales at expenses of dissolving carbonate minerals and biogenic $CaCO_3$ from shells and skeletons.

The NADW is the oldest and most naturally acidic water mass of the studied region. It is located generally below 2500 dbar ($\sigma_2 > 37.00\ kg\ m^{-3}$; Fig. 1b) mainly in the deep Iberian basin and showed weak signs of acidification over the last three decades, although there exist slight differences between the upper and lower NADW branches

BGD
9, 3003–3030, 2012

(uNADW and lNADW). The uNADW is fed by the highly acidic Iceland-Scotland Overflow Water (ISOW) and the LSW. The progressive dilution of these two water masses causes small but observable pH shifts in the comparably much larger volumetric census of the uNADW (Fig. 2). This is particularly noticeable on the uNADW branch incurring into the Iceland basin, under the LSW. The higher influence of LSW/ISOW in the uNADW is revealed by its imprint in the AOU and $Si(OH)_4$ values, which are lower than observed in the lNADW layer (Pérez et al., 2010; Tables S1 and S2 in Supplement). On the other hand the pH of the lNADW was the least affected over time of all inspected water masses. It must be noticed that in this study the lNADW has some influence of Antarctic Bottom Water (AABW). The uNADW is less influenced by AABW than the lNADW, according to the lower silicate concentrations observed in the upper limb when compared to the colder, lower limb of NADW (Tables S1–S3 in Supplement).

The acidic signature of LSW spreading into the Iceland and Eastern North Atlantic (ENA) basins over time responds to several processes. On the one hand, the high phase of the North Atlantic Oscillation (NAO) during the first half of the 1990s prompted in the Irminger basin the formation of a voluminous vintage of CO_2-loaded (and thus more acidic) LSW (Pérez et al., 2008) that later spread into the Iceland and ENA basins (Yashayaev et al., 2008). Later then, the high stratification towards the end of the 1990s (low NAO phase) caused a reduced ventilation and formation rate of LSW that favoured its natural acidification through increased organic matter remineralization and oxygen consumption (Kieke et al., 2007; Pérez et al., 2008), contributing to the observed evolution of pH in the LSW (Fig. 2).

To estimate the acidification rates of the water masses we normalised the discrete in situ pH data to basin-average conditions, condensed the cruise data into averages and removed the natural variability of pH from the direct measurements (Sect. 2.2 and Supplement). In so doing, the resulting acidification trends (Fig. 3) can only be attributed to the anthropogenic forcing. These trends indicated that the upper layers of the NASPG are acidifying faster than the naturally more acidic intermediate and deep waters, due to the increasing atmospheric CO_2 that dissolves first in the surface ocean.

BGD
9, 3003–3030, 2012

The fastest acidification rates corresponded to recently ventilated waters like the Subarctic Intermediate Water (SAIW; $-0.0018 \pm 0.0010\,yr^{-1}$) and the Subpolar Mode Water (SPMW; $-0.0012 \pm 0.0020\,yr^{-1}$). The pH of classical LSW (cLSW) in the Iceland basin presented a remarkable average decrease of $-0.0015 \pm 0.0010\,yr^{-1}$. Any of the former was close to the maximum acidification rates achievable during 1981–2008 that correspond to water masses that were CO_2-equilibrated and kept approximately in pace with the rising atmospheric CO_2 (Dore et al., 2009). On the opposite end we found that the lower NADW (lNADW; Fig. 1b) in the Iberian basin was the least affected by the anthropogenic forcing since only weak pH vs. time correlations with low slopes were obtained ($-0.0002 \pm 0.0002\,yr^{-1}$). The Mediterranean Water (MW) showed a moderate acidification rate ($-0.00047 \pm 0.0008\,yr^{-1}$) in spite of its known capacity for anthropogenic CO_2 (C_{ant}) drawdown from surface layers (Ríos et al., 2001; Álvarez et al., 2005). However, the high specific alkalinity that confers MW the ability to largely neutralise the inputs of C_{ant} can account for this result.

Another general tendency observed is that acidification rates are slower as we move from the Irminger towards the Iberian basin, which is likely due to the increasing buffering capacity (decreasing Revelle Factor – RF) of seawater and to the weakening of convection (compared to the Irminger basin) the further southeast the water parcels are found in the study region. The RF is inversely correlated with temperature and in North Atlantic waters it typically has values of ~10, but higher values of ~12.5 are found in the Irminger Sea (Zeebe and Wolf-Gladrow, 2001; Sabine et al., 2004). A maximum RF of 15.2 has been recently reported for the Iceland Sea as of year 2000 (Olafsson et al., 2009), meaning that for the same amount of CO_2 added to seawater the reduction in pH would be larger in surface waters of the Irminger and Iceland basins than in the ENA basin.

The data analysis also showed that the aragonite lysocline has shoaled at a rate of 7 and $4\,m\,yr^{-1}$ between 1981 and 2008 in the Irminger and Iceland basins, respectively. The latter is in agreement with previous local studies (Olafsson et al., 2009). The fast rate of lysocline shoaling in the Irminger basin is promoted by the intense convection

BGD
9, 3003–3030, 2012

that injects ventilated, CO_2-rich waters into deeper layers (Messias et al., 2008). For comparison sake, the shoaling rates of the lysocline were estimated in ~0.2 m yr^{-1} during the Paleocene-Eocene Thermal Maximum (55 million years ago), when a massive natural release of CO_2 into the atmosphere caused global temperatures to raise more than 5 °C in less than 10 000 yr (Pelejero et al., 2010).

4 Discussion

Although pH normally decreases with increasing depth and dissolved inorganic carbon, such trend appears to be sometimes inverted in the observations. In the Irminger basin for instance (Fig. 3a), the highly ventilated and rapidly formed upper LSW (uLSW) meant a fast injection of surface waters with lower average pH than the deeper cLSW. The formation of uLSW is enhanced during periods of low NAO at expenses of little cLSW production (and vice versa; Corbière et al., 2007), which was the case during the late 1990s (Pérez et al., 2008). Similarly, in the Iceland basin (Fig. 3b) the average pH of cLSW rapidly dropped below that of the upper NADW (uNADW, also known as Northeast Atlantic Deep Water, i.e., NEADW) towards the mid-late 1980s. The high-NAO enhanced ventilation increased the acidification rate and fostered the fast formation of a massive cLSW vintage (compared to uNADW) (Kieke et al., 2007; Yashayaev et al., 2008). The volumetric census of LSW that peaked in the Iceland basin at that time (Pérez et al., 2010) is big enough to invert the regular pH profiles and yield the observed acidification trends. In summary, we conclude that the rapid subduction of newly formed water masses in the NASPG transports the anthropogenic acidification signal into the intermediate waters faster than it would occur only via downward diffusion and mixing of C_{ant}.

It is plausible to make a projection of future pH levels from our set of observations, where the natural component of pH variability has been removed (Sect. 2.2), under certain assumptions. These are that during the next few decades the acidification trends (Fig. 3) and the ocean's general circulation are considered to remain similar to those

BGD
9, 3003–3030, 2012

witnessed during our observation period (last three decades). The SPMW and cLSW are selected for such projection based on the representativeness and relevance of their acidification rates obtained in the Iceland basin (Figs. 2 and 3). They are amongst the most susceptible of the considered water masses to human-induced acidification and have strong pH vs time fits (Fig. 3b). The SPMW represents the highly productive waters of the photic layer and contains one of the largest burdens of anthropogenic CO_2 in the NASPG (Pérez et al., 2010), like the intermediate water cLSW.

One caveat stemming from the above assumptions is that of the prevailing NAO regime that existed between 1981 and 2006, when data was gathered. However, the fact that the NAO phase was close to neutral both in the 1980s and 2000s should minimise such bias. Also, a linear extrapolation of the observed pH trends could be troublesome because it is not constrained, but several works have demonstrated that the decline of carbon system parameters like $[CO_3^{2-}]$ is almost linear for predictions made between 2000 and 2050 (Zeebe and Wolf-Gladrow, 2001; Hauck et al., 2010). Also, this projection is intended for application to surface and intermediate waters on decadal timescales, similar to our observational time span. In so being, the buffering effect of carbonate minerals and biogenic $CaCO_3$ dissolution can be disregarded since this process tends to occur in deep waters over timescales that are at least one order of magnitude larger than the decadal one here considered. On the other hand, the assumption of constant circulation might fall on the conservative side of future acidification scenarios since it will imply that the expected increase of stratification of upper ocean layers (Friedlingstein and Prentice, 2010) be overlooked. The hampered ventilation from increased surface ocean stratification is expected to bring about a decrease in dissolved oxygen concentrations and pH levels, amongst other things because C_{ant} would not be as effectively transported toward the ocean interior via deep convection and water mass formation processes (Pérez et al., 2010).

Under the above assumptions and caveats, a linear extrapolation of the pH trend of decrease similar to the one observed over the last three decades was obtained (Fig. S1 in Supplement). Uncertainties are certainly expected to increase over time as

BGD
9, 3003–3030, 2012

we move away from the observation period. This projection of pH predicts that surface waters in the Iceland basin could undergo a pH drop of ~0.35 units with respect to the pre-industrial era by the time atmospheric CO_2 reaches 800 ppmv, which is consistent with outputs from coupled climate/carbon-cycle models (Caldeira and Wickett, 2005; Orr et al., 2005). Differently though, our estimates for cLSW diverge by about 0.25 pH units with previous model outputs (Caldeira and Wickett, 2003): a pH decrease of more than 0.45 units is expected for cLSW by the time atmospheric CO_2 doubles its present concentration (~775 ppmv; Fig. S1). The notorious difference between model-based and observation-based predictions likely stems from the strong deep convection activity of the North Atlantic that assists the uptake of C_{ant} from the atmosphere. This element of ocean circulation remains elusive to GCMs, at least to the desired level of accuracy. It has also been reported that ocean acidification might be proceeding more rapidly than models have predicted (Wootton et al., 2008), as the contemporary CO_2 emissions are actually exceeding the worst-case scenario forecasts (Canadell et al., 2007; Raupach et al., 2007).

The aragonite saturation state is defined as $\Omega_{arag} = [Ca^{2+}][CO_3^{2-}] \Big/ K'_{sp}$, where square brackets indicate seawater ion concentrations and K'_{sp} is the apparent solubility product of aragonite (Mucci, 1983). Because $[Ca^{2+}]$ is highly and positively correlated with salinity, Ω_{arag} is largely determined by variations in $[CO_3^{2-}]$. This characteristic makes Ω_{arag} an optimum indicator for environmental availability of dissolved carbonate ions. The proposed observation-based projections (Fig. S1 in Supplement) also suggest that it is not surface waters but actually LSW the one that will reach earlier aragonite undersaturation ($\Omega_{arag} < 1$), by the time atmospheric CO_2 reaches ~550 ppmv and not 900 ppmv as suggested by some model predictions (Orr et al., 2005). Depending on our future CO_2 emission rates we could step over the brink of the 550 ppmv by 2050 or even before (Nakicenovic et al., 2000; Caldeira and Wickett, 2005; Feely et al., 2009). Moreover it can be expected that the shoaling of the aragonite lysocline (where $\Omega_{arag} = 1$) will occur quicker in the Irminger than in the Iceland basin, in the light of the

BGD
9, 3003–3030, 2012

faster acidification rates observed (Fig. 3). The upward migration of the lysocline in the NASPG is assisted by the extensive North Atlantic vertical mixing that conveys properties (like C_{ant}) from well-ventilated surface waters to deeper ocean layers (Messias et al., 2008). The shoaling of the isopleth $\Omega_{arag} = 1$ is likely to occur in progressively longer pulses that will eventually come to year-round lasting effects but would, nevertheless, be sensed during late wintertime in the first stages of lysocline shoaling. At that time of the year the sea surface temperatures reach the annual minimum, wind-driven mixing and seawater pCO_2 values are highest, and surface waters outcrop into the winter mixed layer (Olafsson et al., 2009; Dore et al., 2009; Vázquez-Rodríguez et al., 2012).

Altogether, the low buffering capacity of the NASPG (Sabine et al., 2004), the fast acidification rates of the SPMW and LSW (Fig. 3) and the rapid shoaling of the lysocline (Gattuso et al., 1998) in the Iceland basin can affect cold-water corals (Tittensor et al., 2010) as well as other calcifying organisms (Gattuso et al., 1999; Gazeau et al., 2007; Comeau et al., 2009). Cold-water corals are slow growing (4–25 mm yr^{-1}), long-lived (>8000 yr) calcifying species that build around them fragile ecosystems of phenomenal biodiversity (Roberts et al., 2006; Wheeler et al., 2011) and serve as nurseries for a large number of commercial and non-commercial species (Raven et al., 2005; Doney et al., 2009; Hoffman et al., 2010). Because they dwell in regions where natural pH shifts are very small it can be expected that the effects of anthropogenic acidification will be more severe for these communities than for their warm-water cousins (Guinotte et al., 2006; Rodolfo-Metalpa et al., 2010; Pandolfi et al., 2011; Wheeler et al., 2011). It is difficult for the time being to know and assess the full spectrum of consequences from CO_2-induced acidification in these habitats (Doney et al., 2009; Hoffman et al., 2010; Tittensor et al., 2010), since the research field of the effects of acidification on calcifying organisms is still in its infancy (Gattuso et al., 2009). However, it is expected that the physiological fitness of calcifying organisms will be substantially affected (Guinotte et al., 2006).

BGD
9, 3003–3030, 2012

5 Conclusions

The progressive acidification of North Atlantic waters has been assessed from in situ pH measurements and other carbon system parameters spanning the last three decades. The increasing atmospheric CO_2 concentrations have largely affected the pH of surface and deep waters in the three studied North Atlantic regions, at varying extents. Most importantly, the LSW has shown acidification rates higher than expected that are amongst the highest ones in the NASPG. As expected (Byrne et al., 2010), surface waters show the highest acidification rates in spite of the active biologic removal of carbonic acid species through photosynthesis. The SAIW has the fastest of these rates ($-0.0018 \pm 0.0001\ yr^{-1}$). The weaker convection activity and deeper bathymetry of the ENA basin account for the lower acidification rates obtained in this region. Predictions from an observation-based extrapolation of current acidification trends and rates are in agreement with model results (Caldeira and Wickett, 2005; Orr et al., 2005) in surface layers. However, our results indicate that the intermediate waters of the North Atlantic (LSW in particular) are getting acidified more rapidly than what GCMs predicted. Guinotte et al. (2006) have in fact pointed out that some deep-sea cold-water corals may experience undersaturated waters as early as 2020 under an IPCC "business-as-usual" CO_2 emission pathway, which is in good agreement with our observation-based results for the Iceland and Irminger basins.

Supplementary material related to this article is available online at: http://www.biogeosciences-discuss.net/9/3003/2012/bgd-9-3003-2012-supplement.pdf.

Acknowledgements. The authors wish to thank C. Pelejero for his comments. This work was funded an developed under the European Commission within the 7th Framework Programme EU FP7-ENV-2010 CARBOCHANGE Collaborative Project (Contract no. 264879), the Spanish Ministry of Sciences and Innovation project CATARINA (CTM2010-17141) and Acción Integrada Hispano-Francesa (HF2006-0094). The OVIDE research project was co-funded by the

BGD
9, 3003–3030, 2012

IFREMER, CNRS/INSU and LEFE. H. M. was supported by CNRS. M. V. R. was funded by CSIC I3P Predoctoral Grant program (I3P-BPD2005).

References

Álvarez, M., Pérez, F. F., Shoosmith, D. R., and Bryden, H. L.: The unaccounted role of Mediterranean Water in the draw-down of anthropogenic carbon, J. Geophys. Res., 110, 1–18, doi:10.1029/2004JC002633, 2005.

Azetsu-Scott, K., Jones, E. P., Yashayaev, I., and Gershey, R. M.: Time series study of CFC concentrations in the Labrador Sea during deep and shallow convection regimes (1991–2000), J. Geophys. Res., 108, 3354, doi:10.1029/2002JC001317, 2003.

Bradshaw, A., Brewer, P., Shafer, D., and Williams, R.: Measurements of total carbon dioxide and alkalinity by potentiometric titration in the GEOSECS program, Earth Planet. Sci. Lett., 55, 99–115, 1981.

Byrne, R. H., Mecking, S., Feely, R. A., and Liu, X.: Direct observations of basin-wide acidification of the North Pacific Ocean, Geophys. Res. Lett., 37, L02601, doi:10.1029/2009GL040999, 2010.

Caldeira, K. and Wickett, M. E.: Anthropogenic carbon and ocean pH, Nature, 425, 365, 2003.

Caldeira, K. and Wickett, M. E.: Ocean model predictions of chemistry changes from carbon dioxide emissions to the atmosphere and ocean, J. Geophys. Res., 110, C09S04, doi:10.1029/2004JC002671, 2005.

Canadell, J., LeQuéré, C., Raupach, M. R., Fields, C., Buitenhuis, E. T., Ciais, P., Conway, T. J., Gillett, N. P., Houghton, R. A., and Marland, G.: Contributions to accelerating atmospheric CO_2 growth from economic activity, carbon intensity, and efficiency of natural sinks, Proc. Natl. Acad. Sci., 104, 18866–18870, doi:10.1073/pnas.0702737104, 2007.

Clayton, T. D. and Byrne, R. H.: Calibration of m-cresol purple on the total hydrogen ion concentration scale and its application to CO_2-system characteristics in seawater, Deep-Sea Res., Part I, 40, 2115–2129, 1993.

Comeau, S., Gorsky, G., Jeffree, R., Teyssié, J.-L., and Gattuso, J.-P.: Impact of ocean acidification on a key Arctic pelagic mollusc (Limacina helicina), Biogeosciences, 6, 1877–1882, doi:10.5194/bg-6-1877-2009, 2009.

Corbière, A., Metzl, N., Reverdin, G., Brunet, C., and Takahashi, T.: Interannual and decadal

BGD
9, 3003–3030, 2012

variability of the oceanic carbon sink in the North Atlantic subpolar gyre, Tellus, 59, 168–178, doi:10.1111/j.1600-0889.2006.00232.x, 2007.
Dickson, A. G.: The measurement of sea water pH, Mar. Chem., 44, 131–142, 1993.
Dickson, A. G. and Millero, F. J.: A comparison of the equilibrium constants for the dissociation of carbonic acid in seawater media, Deep-Sea Res., Part I, 34, 1733–1743, 1987.
Dickson, A. G., Sabine, C. L., and Christian, J. R. (Eds.): Guide to best practices for ocean CO_2 measurements. PICES Special Publication 3, 191 pp., 2007.
Doney, S. C., Fabry, V. J., Feely, R. A., and Kleypas, J. A.: Ocean Acidification: The Other CO_2 Problem, Annu. Rev. Marine, 1, 169–192, 2009.
Dore, J. E., Lukas, R., Sadler, D. W., Church, M. J., and Karl, D. M.: Physical and biogeochemical modulation of xCO North Pacific, Proc. Natl. Acad. Sci., 106, 12235–12240, 2009.
Fabry, V. O. J., McClintock, J. B., Mathis, J. T., and Grebmeier, J. M.: Ocean acidification at high latitudes: The Bellwether, Oceanography, 22, 160–171, 2009.
Feely, R. A., Sabine, C. L., Lee, K., Berelson, W., Kleypas J., Fabry, V. J., and Millero, F. J.: Impact of anthropogenic CO_2 on the $CaCO_3$ system in the oceans, Science, 305, 362–366, 2004.
Feely, R. A., Sabine, C. L., Hernandez-Ayon, J. M., Ianson, D., and Hales, B.: Evidence for upwelling of corrosive "acidified" water onto the continental shelf, Science, 320, 1490–1492, 2008.
Feely, R. A., Doney, S. C., and Cooley, S. R.: Ocean acidification: present conditions and future changes in a high-CO_2 world, Oceanography, 22, 160–171, 2009.
Friis, K., Koertzinger, A., and Wallace, D. W. R.: Spectrophotometric pH measurement in the ocean: requirements, design and testing of an autonomous charge-coupled device detector system, Limnol. Oceanogr.-Meth., 2, 126–136, 2004.
Friis, K., Koertzinger, A., Patsch, J., and Wallace, D. W. R.: On the temporal increase of anthropogenic CO_2 in the subpolar North Atlantic, Deep-Sea Res., Part I, 52, 681–698, 2005.
Friedlingstein, P. and Prentice I. C.: Carbon-climate feedbacks: a review of model and observation based estimates, Curr. Opin. Environ. Sust., 2, 251–257, doi:10.1016/j.cosust.2010.06.002, 2010.
Friedlingstein, P., Cox, P., Betts, R., Bopp, L., von Bloh, W., Brovkin, V., Cadule, P., Doney, S., Eby, M., Fung, I., Bala, G., John, J., Jones, C., Joos, F., Kato, T., Kawamiya, M., Knorr, M., Lindsay, K., Matthews, H. D., Raddatz, T., Rayner, P., Reick, C., Roeckner, E., Schnitzler, K.-G., Schnur, R., Strassmann, K., Weaver, A. J., Yoshikawa, C., and Zeng, N.: Climate-

BGD
9, 3003–3030, 2012

carbon cycle feedback analysis: results from the C4MIP model intercomparison, J. Climate, 19, 3337–3353, 2006.
Gattuso, J.-P. and Lavigne, H.: Technical Note: Approaches and software tools to investigate the impact of ocean acidification, Biogeosciences, 6, 2121–2133, doi:10.5194/bg-6-2121-2009, 2009.
Gattuso, J.-P., Frankignoulle, M., Bourge, I., Romaine, S., and Buddemeier, R. W.: Effect of calcium carbonate saturation of seawater on coral calcification, Global Planet. Change, 18, 37–46, 1998.
Gattuso, J.-P., Allemand, D., and Frankignoulle, M.: Photosynthesis and calcification at cellular, organismal and community levels in coral reefs: a review on interactions and control by carbonate chemistry, Am. Zool., 39, 160–183, 1999.
Gazeau, F., Quiblier, C., Jansen, J. M., Gattuso, J.-P., Middelburg, J. J., and Heip, C. H. R.: Impact of elevated CO_2 on shellfish calcification, Geophys. Res. Lett., 34, L07603, doi:10.1029/2006GL028554, 2007.
Hofmann, G. E., Barry, J. P., Edmunds, P. J., Gates, R. D., Hutchins, D. A., Klinger, T., and Sewell, M. A.: The Effect of Ocean Acidification on Calcifying Organisms in Marine Ecosystems: An Organism to Ecosystem Perspective, Annu. Rev. Ecol. Evol. Syst., 41, 127–47, 2010.
Guinotte, J. M., Orr, J., Cairns, S., Freiwald, A., Morgan, L., and George, R.: Will human-induced changes in seawater chemistry alter the distribution of deep-sea scleractinian corals?, Front. Ecol. Environ., 4, 141–146, 2006.
Hauck, J., Hoppema, M., Bellerby, R. G. J., Völker, C., and Wolf-Gladrow, D.: Data-based estimation of anthropogenic carbon and acidification in the Weddell Sea on a decadal timescale, J. Geophys. Res., 115, C03004, doi:10.1029/2009JC005479, 2010.
Hönisch, B., Ridgwell, A., Schmidt, D. N., Thomas, E., Gibbs, S. J., Sluijs, A., Zeebe, R., Kump, L., Martindale, R. C., Greene, S. E., Kiessling, W., Ries, J., Zachos, J. C., Royer, D. L., Barker, S., Marchitto Jr., T. M., Moyer, R., Pelejero, C., Ziveri, P., Foster, G. L., and Williams, B.: The Geological Record of Ocean Acidification, Science, 335, 1058–1063, 2012.
Ilyina, T., Zeebe, R., and Brewer, P.: Changes in underwater sound propagation caused by ocean acidification, IOP Conf. Series: Earth Env. Sci., 6, 462007, doi:10.1088/1755-1307/6/6/462007, 2009.
Johnson, K. M., Wills, K. D., Butler, D. B., Johnson, W. K., and Wong, C. S.: Coulometric total carbon dioxide analysis for marine studies: Maximizing the performance of an automated

BGD
9, 3003–3030, 2012

continuous gas extraction system and coulometric detector, Mar. Chem., 44, 167–189, 1993.
Khatiwala, S., Primeau, F., and Hall, T.: Reconstruction of the history of anthropogenic CO_2 concentrations in the ocean, Nature, 462, 346–349 doi:10.1038/nature08526, 2009.
Kieke, D., Rhein, M., Stramma, L., Smethie, W. M., Bullister, J. L., and LeBel, D. A.: Changes in the pool of Labrador Sea Water in the subpolar North Atlantic, Geophys. Res. Lett., 34, L06605, doi:10.1029/2006GL028959, 2007.
Messias, M. J., Watson, A. J., Johannessen, T., Oliver, K. I. C., Olsson, K. A., Fogelqvist, E., Olafsson, J., Bacon, S., Balle, J., Bergman, N., Budéus, G., Danielsen, M., Gascard, J. C., Jeansson, E., Olafsdottir, S. R., Simonsen, K., Tanhua, T., Scoy, K. V., and Ledwell, J. R.: The Greenland Sea tracer experiment 1996–2002: Horizontal mixing and transport of Greenland Sea Intermediate Water, Prog. Oceanogr., 78, 85–105, 2008.
Millero, F. J.: The marine inorganic carbon cycle, Chem. Rev. 107, 308–341, 2007.
Millero, F. J., Zhang, J. Z., Lee, K., and Campbell, D. M.: Titration alkalinity of seawater, Mar. Chem., 44, 153–156, 1993.
Mintrop, L., Perez, F. F., Gonzalez-Davila, M., and Santana-Casiano, M. J., and Kortzinger, A.: Alkalinity determination by potentiometry: Intercalibration using three different methods, Cienc. Mar., 26, 23–37, 2002.
Mucci, A.: The solubility of calcite and aragonite in sea water at various salinities, temperatures and one atmosphere total pressure, Am. J. Sci., 238, 780–799, 1983.
Nakicenovic, N., Alcamo, J., Davis, G., de Vries, B., Fenhann, J., Gaffin, S., Gregory, K., Grubler, A., Jung, T. Y., Kram, T., La Rovere, E. L., Michaelis, L., Mori, S., Morita, T., Pepper, W., Pitcher, H., Price, L., Raihi, K., Roehrl, A., Rogner, H.-H., Sankovski, A., Schlesinger, M., Shukla, P., Smith, S., Swart, R., van Rooijen, S., Victor, N., and Dadi, Z.: IPCC Special Report on Emissions Scenarios, Cambridge University Press, Cambridge, United Kingdom and New York, NY, USA, 599 pp., 2000.
Olafsson, J., Olafsdottir, S. R., Benoit-Cattin, A., Danielsen, M., Arnarson, T. S., and Takahashi, T.: Rate of Iceland Sea acidification from time series measurements, Biogeosciences, 6, 2661–2668, doi:10.5194/bg-6-2661-2009, 2009.
Orr, J. C., Fabry, V. J., Aumont, O., Bopp, L., Doney, S. C., Feely, R. A., Gnanadesikan, A., Gruber, N., Ishida, A., Joos, F., Key, R. M., Lindsay, K., Maier-Reimer, E., Matear, R., Monfray, P., Mouchet, A., Najjar, R. G., Plattner, G.-K., Rodgers, K. B., Sabine, C. L., Sarmiento, J. L., Schlitzer, R., Slater, R. D., Tot- terdell, I. J., Weirig, M. F., Yamanaka, Y., and Yool, A.: Anthropogenic ocean acidification over the twenty-first century and its impact on calcifying

BGD
9, 3003–3030, 2012

organisms, Nature, 437, 681–686. doi:10.1038/nature04095, 2005.
Pandolfi, J. M., Connolly, S. R., Marshall, D. J., and Cohen, A. L.: Projecting Coral Reef Futures Under Global Warming and Ocean Acidification, Science, 333, 418–422, 2011.
Pelejero, C., Calvo, E., and Hoegh-Guldberg, O.: Paleo-perspectives on ocean acidification, Trends Ecol. Evol., 25, 332–344, 2010.
Pérez, F. F. and Fraga, F.: A precise and rapid analytical procedure for alkalinity determination, Mar.Chem., 21, 169–182, 1987.
Pérez, F. F., Vázquez-Rodrguez, M., Louarn, E., Padín, X. A., Mercier, H., and Ríos, A. F.: Temporal variability of the anthropogenic CO_2 storage in the Irminger Sea, Biogeosciences, 5, 1669–1679, doi:10.5194/bg-5-1669-2008, 2008.
Pérez, F. F., Vázquez-Rodríguez, M., Mercier, H., Velo, A., Lherminier, P., and Ríos, A. F.: Trends of anthropogenic CO_2 storage in North Atlantic water masses, Biogeosciences, 7, 1789–1807, doi:10.5194/bg-7-1789-2010, 2010.
Raupach, M. R., Marland, G., Ciais, P., LeQuéré, C., Canadell, J. G., Klepper, G., and Field, C. B.: Global and regional drivers of accelerating CO_2 emissions, Proc. Natl. Acad. Sci. USA, 104, 10288–10293, 2007.
Raven, J., Caldeira, K., Elderfield, H., Hoegh-Guldberg, O., Liss, P., Riebesell, U., Shepherd, J., Turley, C., and Watson, A.: Ocean acidification due to increasing atmospheric carbon dioxide, Policy document 12/05, The Royal Society, London, 2005.
Ríos, A. F., Pérez, F. F., and Fraga, F.: Long term (1977–1997) measurements of carbon dioxide in the Eastern North Atlantic: evaluation of anthropogenic input, Deep-Sea Res., Part II, 48, 2227–2239, 2001.
Roberts J. M., Wheeler, A. J., and Freiwald, A.: Reefs of the deep: the biology and geology of cold-water coral ecosystems, Science, 312, 543–47, 2006.
Rodolfo-Metalpa, R., Martin, S., Ferrier-Pagès, C., and Gattuso, J.-P.: Response of the temperate coral Cladocora caespitosa to mid- and long-term exposure to pCO_2 and temperature levels projected for the year 2100 AD, Biogeosciences, 7, 289–300, doi:10.5194/bg-7-289-2010, 2010.
Sabine, C. L., Feely, R. A., Gruber, N., Key, R. M., Lee, K., Bullister, J. L., Wanninkhof, R., Wong, C. S., Wallace, D. W. R., Tilbrook, B., Millero, F. J., Peng, T.-H., Kozyr, A., Ono, T., and Ríos, A. F.: The oceanic sink for anthropogenic CO_2, Science, 305, 367–371, 2004.
Tittensor, D. P., Baco, A. R., Hall-Spencer, J. M., Orr, J. C., and Rogers, A. D.: Seamounts as refugia from ocean acidification for cold-water stony corals, Mar. Ecol., 31, 212–225,

BGD
9, 3003–3030, 2012

doi:10.1111/j.1439-0485.2010.00393.x, 2010.
Vázquez-Rodríguez, M., Padin, X. A., Pardo, P. C., Ríos, A. F., and Pérez, F. F.: The subsurface layer reference to calculate preformed alkalinity and air-sea CO_2 disequilibrium in the Atlantic Ocean, J. Marine Syst., 94, 52–63, 2012.
Wheeler, A. J., Kozachenko, M., Henry, L.-A., Foubert, A., de Haas, H., Huvenne, V. A. I., Masson, D. G., and Olu, K.: The Moira Mounds, small cold-water coral banks in the Porcupine Seabight, NE Atlantic: Part A – an early stage growth phase for future coral carbonate mounds?, Mar. Geol., 282, 53–64, 2011.
Wootton, J. T., Pfister, C. A., and Forester, J. D.: Dynamic patterns and ecological impacts of declining ocean pH in a high-resolution multi-year dataset, Proc. Natl. Acad. Sci. 105, 18848–18853, 2008.
Yashayaev, I., Penny Holliday, N., Bersch, M., and van Aken, H. M.: The history of the Labrador Sea Water: Production, Spreading, Transformation and Loss, in: "Arctic-Subarctic Ocean Fluxes: defining the role of the Northern Seas in climate", edited by: Robert, R., Dickson, J., and Meincke, P., Rhines, Springer, P.O. Box 17, 3300 AA Dordrecht, The Netherlands, 569–612, 2008.
Zeebe R. E. and Wolf-Gladrow D.: CO_2 in Seawater: Equilibrium, Kinetics, Isotopes. Amsterdam: Elsevier Science, B.V., 346 pp., 2001.

BGD
9, 3003–3030, 2012

Table 1. List of selected North Atlantic cruises (Fig. 1a). Acronyms denote: P.I. = principal investigator; #St = number of stations; #Sp = number of samples; *S* = variable measured with spectrophotometric techniques; *P* = variable measured with potentiometric techniques; C = pH calculated from C_T and A_T using the thermodynamic equations of the carbon system (Dickson et al., 2007) and a set of carbon dioxide dissociation constants (Dickson and Millero, 1987); n.a. = no adjustment made. The analytical precision limits of spectrophotometric and potentiometric pH measurements were assessed in ±0.002 and ±0.005, respectively. In the case of pH data calculated from C_T and A_T (pH "C"), the associated pH errors are ±0.004, except in the TTO cruise (±0.008). Adjustments from a posterirori crossover analysis are listed in µmol kg^{-1} for C_T and A_T.

	Cruises and pH measurements						Adjustments		
Section	Year	P.I.	Expocode	#St	#Sp	pH	pH	C_T	A_T
TTO	1981	T. Takahashi	316N19810923	30	591	C	n.a.	−3.0	−3.6
BD3	1989	M. Arhan	35LU19890509	20	218	P	0.024	n.a.	n.a.
TYRO	1990	G. Fransz	64TR19900417	11	189	C	n.a.	n.a.	14
AR07E	1991	H. M. van Aken	64TR19910408	30	616	C	n.a.	6	n.a.
A01E	1991	J. Meincke	06MT18_1	26	431	C	n.a.	n.a.	n.a.
OACES	1993	R. Wanninkhof	OACES93	28	497	C	n.a.	n.a.	n.a.
FOUREX	1997	S. Bacon	74DI19970807	83	1458	S	−0.005	n.a.	n.a.
MET97	1997	F. Schott	06MT19970707	8	148	C	n.a.	n.a.	n.a.
CHAOS	1998	Smythe – Wright	74DI19980423	26	459	S	0.018	n.a.	−8.5
OVIDE 2002	2002	H. Mercier	35TH20020611	85	1829	S	n.a.	n.a.	n.a.
A16N	2003	J. Bullister – N. Gruber	33RO20030604	25	693	C	n.a.	n.a.	n.a.
OVIDE 2004	2004	T. Huck	35TH20040604	98	2091	S	n.a.	n.a.	n.a.
OVIDE 2006	2006	P. Lherminier	06M220060523	89	1937	S	n.a.	n.a.	n.a.
OVIDE 2008	2008	B. Ferron	35TH20080610	87	2012	S	n.a.	n.a.	n.a.

BGD
9, 3003–3030, 2012

Table 2. List of coefficients obtained for Eq. (1) using the expression in Eq. (2) in each water mass and basin. "ENA" stands for Eastern North Atlantic. Between brackets are the properties associated to each "a_i" coefficient and the corresponding units. All "a_i" coefficients have been scaled up by a factor of 10^3, except for the salinity ones ("a_5"). The "n.s." ("not significant") variables explained very little of the pH variability and weakened the overall MLR fit so they were therefore rejected according to a stepwise method of MLR solving.

Water Mass	R^2	a_1 ($Si(OH)_4$; $kg \cdot \mu mol^{-1}$)	a_2 (AOU; $kg \cdot \mu mol^{-1}$)	a_3 (θ; $^\circ C^{-1}$)	a_4 (S)	a_5 (xCO_2; ppm^{-1})
			Irminger Basin			
SAIW	0.97	-15 ± 2	n.s.	n.s	0.18 ± 0.03	-1.02 ± 0.08
*u*LSW	0.99	-11 ± 1	n.s.	30 ± 10	0.67 ± 0.08	-0.95 ± 0.04
cLSW	0.99	-17 ± 3	n.s.	97 ± 16	0.44 ± 0.11	-0.50 ± 0.04
uNADW	0.89	n.s.	n.s.	n.s.	n.s.	-0.56 ± 0.07
DSOW	0.78	n.s.	n.s.	n.s.	n.s.	-0.57 ± 0.12
			Iceland Basin			
SPMW	0.94	n.s.	-1.5 ± 0.3	17 ± 3	n.s.	-0.61 ± 0.15
*u*LSW	0.96	-7 ± 2	n.s.	n.s.	n.s.	-0.72 ± 0.06
cLSW	0.81	-11 ± 6	n.s.	-40 ± 24	n.s.	-0.95 ± 0.21
uNADW	0.75	n.s.	2 ± 1	n.s.	-0.8 ± 0.4	-0.53 ± 0.16
			ENA Basin			
NACW	0.89	n.s.	-1.0 ± 0.4	11 ± 2	n.s.	-0.54 ± 0.09
MW	0.96	n.s.	-1.0 ± 0.2	15 ± 3	n.s.	-0.26 ± 0.07
LSW	0.77	n.s.	n.s.	n.s.	n.s.	-0.42 ± 0.08
uNADW	0.78	n.s.	-2.3 ± 0.6	270 ± 110	-3 ± 1	n.s.
lNADW	0.28	n.s.	n.s.	200 ± 130	n.s.	0.13 ± 0.10

BGD
9, 3003–3030, 2012

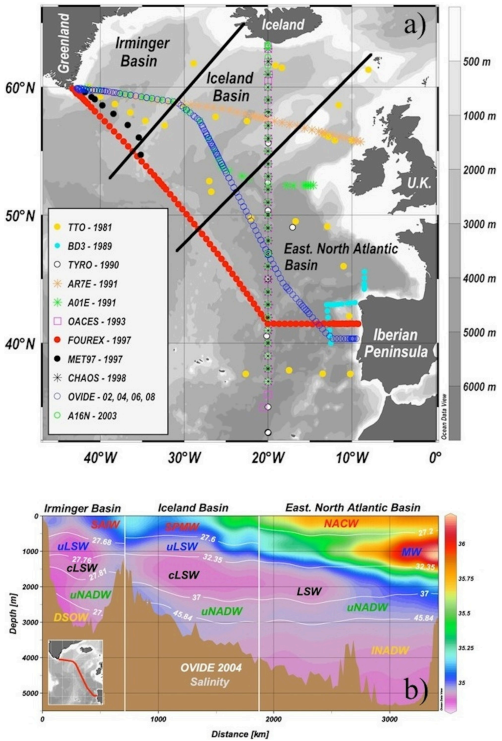

Fig. 1. **(a)** shows the study area and selected cruises. The black straight lines delimit the Irminger, Iceland and Eastern North Atlantic (ENA) basins. **(b)** shows the main NASPG water masses considered for this study over the salinity distribution of the OVIDE 2004 section, which gives representative coverage of the NASPG. The isopycnals represent density anomalies (σ; kg m^{-3}). The acronyms stand for: SAIW = Sub Arctic Intermediate Water; LSW = Labrador Sea Water; NADW = North Atlantic Deep Water; SPMW = Sub Polar Mode Water; NACW = North Atlantic Central Water; MW = Mediterranean Water. The lowercase first letters "c", "u" and "l" denote "classical", "upper" and "lower", respectively.

BGD
9, 3003–3030, 2012

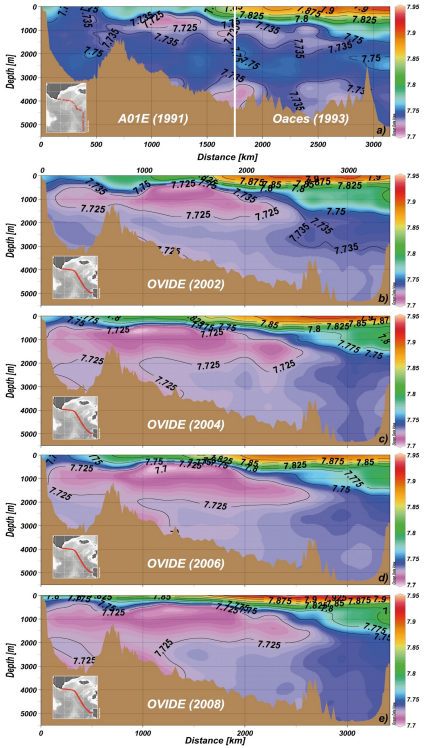

Fig. 2. The evolution of measured pH distributions in the NASPG. The x-axis represents transect distances (km) from the southernmost tip of Greenland towards the Iberian Basin. The section in **(a)** is a composite of the A01E and OACES cruises that matches closely the OVIDE section (Fig. 1a) that extends further back in time the comparison of pH values. The two-year difference between the A01E and OACES cruises is assumable compared with the nine-year gap between this composite section and the OVIDE 2002 cruise **(b)**. This assumption is also supported by continuum of pH fields in intermediate and deep waters at the merging line.

BGD
9, 3003–3030, 2012

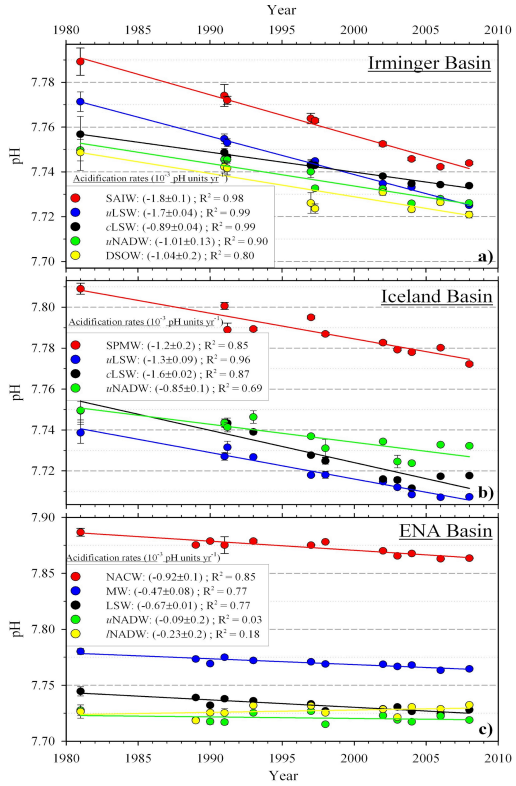

Fig. 3. Trends and rates of anthropogenic acidification between 1981 and 2008 of the studied water masses in the Irminger basin **(a)**, Iceland basin **(b)** and ENA basin **(c)**. Acidification rates (in 10^{-3} pH units yr^{-1}) and correlation coefficients (R^2) of the fits are given in the legend. Each of the points in the scatter plots represents the average pH of a particular water mass in each basin at the time the cruises were conducted. Considering the ample time interval (1981–2008) these pH averages represent well annual means. The error bars are the standard errors of the mean.

BGD
9, 3003–3030, 2012